Implementation of an autocorrelation-based spectrum sensing algorithm in real-world channels with frequency offset

Pat Chambers
Institute of Sensors, Signals and Systems
School of Engineering and Physical Sciences
Heriot-Watt University
Edinburgh, EH14 4AS, UK.
Email: p.chambers@surrey.ac.uk

Mathini Sellathurai
Institute of Sensors, Signals and Systems
School of Engineering and Physical Sciences
Heriot-Watt University
Edinburgh, EH14 4AS, UK.
Email: M.Sellathurai@hw.ac.uk

***Abstract*—This work presents a testbed implementation of a spectrum sensing algorithm for cognitive radio that is based on the autocorrelation function. Much of the work in current literature uses simulation based approaches to characterize functionality. In contrast here, the algorithm is applied in real-world channels and compared with appropriate simulations. It is shown how the algorithm may be improved to overcome the problem of frequency offset, which is a hardware-based impairment that current literature on the algorithm generally does not consider.**

I. Introduction

Cognitive radio (CR) is a novel communications technique that better utilises the available elctromagnetic spectrum by dynamically adapting the transmission and receive signaling parameters to suit the behaviour of the radio environment. Considering primarily the receiver in a CR system, the initial and most important stage is that of spectrum sensing, which involves the receiver determining whether there is a signal present at a certain carrier frequency and time instant or not. The simplest means to do this is to use an energy detector [1], which is a circuit that can detect signal power using very low complexity techniques. However, energy detectors exhibit very poor performance at low SNR and also have the disadvantage of not being able to make any distinction between different types of signal. To overcome this limitation, a recent technique that exploits the cyclostationarity of orthogonal frequency division multiplexing (OFDM) signals has been described [2] [3]. The cyclostationarity occurs due to the fact that OFDM employs a cyclic prefix (CP), which is repetition of a collection of data signal samples, which occur at the end of block, at the start of the block. Since the length of the CP portion and data samples portion of the block varies according to the type of OFDM signal employed, so too does the nature of the cyclostationarity. An algorithm that can be used to test for this pattern is the autocorrelation-based spectrum sensing or feature detecting algorithm. The basic principal is to assume a certain pattern of cyclostationarity and then perform an autocorrelation on the signal and determine whether there is a noticeable peak or not by comparing with an appropriately determined threshold. The length of data samples portion of the OFDM block is equivalent to the fast Fourier transform (FFT) employed in implementing the particular type of OFDM. Thus if an incorrect FFT size is assumed or if only added white Gaussian noise (AWGN) samples are present, then the threshold will not be exceeded and hence the test fails. Further, by cycling though various FFT sizes at the receiver appropriately, the type of OFDM signal (or presence of AWGN) can be determined. The complexity of this type of spectrum sensing technique is relatively low making it an attractive option for implementation and a comparative review of this algorithm and other types of spectrum sensing technique may be found in [4].

In literature, there exist few publications with regard to physical implementation of this algorithm, with most work focusing on simulation-based performance characterisation. However in [5], a field programmable gate array (FPGA) approach to implementation was proposed and the effect of direct current (DC) offset was examined and was shown to be a significant impairment if present. An issue with this approach however, was that only relatively small FFT sizes were considered. In contrast in this work, an extension to this implementation is proposed, whereby the algorithm can function larger FFT sizes by overcoming the problem of frequency offset.

This paper is organised as follows. In Section II, the algorithm system model is presented and in Section III, the signal parameters along with the testbed implementation hardware are described. Section IV outlines the problem of frequency offset the proposed algorithm improvement. Results are presented in Section V with concluding remarks in Section VI.

II. System model

The goal of the autocorrelation detector is to distinguish between AWGN samples and OFDM signal samples, which have similar statistical properties. This may be summarised by the following hypothesis test in relation to a received signal, $y(t)$:

$$\left.\begin{array}{l} H_0 : y(t) = n(t) \\ H_1 : y(t) = x(t) + n(t) \end{array}\right\} \quad y(t) \sim \mathcal{N}_{\mathrm{c}}\left(0, \sigma_y^2\right). \qquad (1)$$

Pat Chambers is now with the Centre for Communications Systems Research (CCSR), University of Surrey, Guildford, Surrey, GU2 7XH, UK.

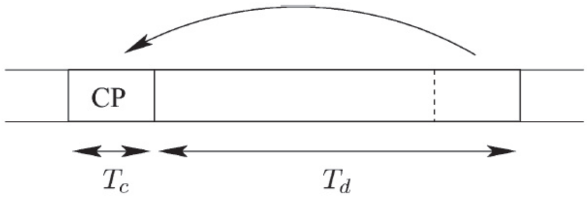

Fig. 1. OFDM block structure [6].

H_0 refers to the null hypothesis, which is effectively the detection of AWGN samples, i.e., $n(t)$, and H_1 is the alternate hypothesis, which is the detection of a combination of OFDM symbols and AWGN samples, i.e., $x(t) + n(t)$. The notation $\sim \mathcal{N}_c(\mu, \sigma^2)$ denotes the complex Gaussian distribution with mean, μ, and variance, σ^2, which, as indicated previously, clearly applies for the case of both hypotheses. In order to be able to distinguish between these two hypotheses, particularly at low SNR, it is necessary to develop an appropriate test statistic and compare it to a similarly appropriate threshold in order to make a decision about the nature of the received samples, $y(t)$.

The structure of an OFDM block is now depicted in Fig. 1. It consists partly of a series of T_d samples, which constitute the useful data bearing length of the block and are derived from the inverse fast fourier transform (IFFT) of a series complex modulation symbols. The FFT size used in the OFDM signal and T_d are equivalent numerically. It also consists of a CP, which is a series of T_c samples that are a replication of a number of samples taken from the end of series, T_d. The main purpose of the CP is to facilitate orthogonality of the modulation symbols in the frequency domain at the receiver by converting the Toeplitz convolutional structure of the channel to a circulant one. However, in statistical terms, the implementation of the CP means that the OFDM block exhibits cyclostationarity and, as a result, there is peak in the autocorrelation function when it is applied to a set of OFDM samples of minimum length $2T_d + T_c$ when the lag is set T_d. From this idea, a test statistic, ρ, has been derived that is a maximum likelihood estimate (MLE) of the autocorrelation coefficient of $y(t)$ at lag T_d, which may be written as [2] [3]:

$$\rho = \frac{\frac{1}{2M}\sum_{t=0}^{M-1} \Re\left\{y(t)\, y^*(t+T_d)\right\}}{\frac{1}{2M+T_d}\sum_{t=0}^{M+T_d-1} |y(t)|^2}. \qquad (2)$$

$\Re\{\cdot\}$ and $(\cdot)^*$ denote the real part of a complex number and the complex conjugate respectively. M is the number of receive samples recorded that is generally accepted to be a number greater than $2T_d + T_c$. It was shown in [6] that ρ under the null hypothesis is distributed according to:

$$H_0 : \rho \sim \mathcal{N}_R\left(0, \frac{1}{2M}\right), \qquad (3)$$

where $\sim \mathcal{N}_R$ refers to the Gaussian distribution for real valued numbers. Given that due to its Gaussian statistics, ρ has a probability of exceeding an arbitrary threshold, η_ρ, that may be expressed as: $P(\rho > \eta_\rho) = \frac{1}{2}\operatorname{erfc}\left(\frac{\eta_\rho}{\sqrt{2}\sigma_r}\right)$, with $\operatorname{erfc}(\cdot)$ denoting the complimentary error function, it now follows that:

$$P(\rho > \eta_\rho | H_0) = \frac{1}{2}\operatorname{erfc}\left(\sqrt{M}\eta_\rho\right). \qquad (4)$$

From eqn (3), it is known that the expected value of ρ under the null hypothesis is zero thus the term $P(\rho > \eta_\rho | H_0)$ may be thought of as a probability of false alarm, P_{fa}, in the context of detecting AWGN samples. Thus given the test statistic, ρ, it is now possible to derive an appropriate threshold η_ρ, based on a tolerable specified level of false alarm, P_{fa}, as:

$$\eta_\rho = \frac{1}{\sqrt{M}}\operatorname{erfc}^{-1}(2P_{fa}). \qquad (5)$$

In in order to construct a detector to distinguish between either hypothesis in eqn (1), many successive recordings of $y(t)$ are made, each of which is M samples long, and ρ is appropriately compared with the threshold η_ρ.

TABLE I. OFDM SIGNAL PARAMETERS.

Parameter	WiMAX	LTE 5 MHz	LTE 20 MHz
Modulation scheme	16 QAM	16 QAM	16 QAM
Data/FFT size, T_d	256	512	2048
CP size, T_c	64	32	144
$T_c/(T_d + T_c)$	0.2	0.0657	0.0657
Sub-carrier spacing, Δf	22.5 kHz	15 kHz	15 kHz
Sampling rate, F_s	5.76 MHz	7.68 MHz	30.72 MHz
Bandwidth, BW	5 MHz	5 MHz	20 MHz
$M - T_d$	1472	2668	10672
Sensing time	0.255 ms	0.347 ms	0.347 ms
Sensing time w/FFO correction	12.5 ms	17.4 ms	17.4 ms

III. Signals and Testbed

In order to verify this algorithm experimentally, various OFDM signals in conjunction with a wireless testbed are employed. These OFDM signals are now described before the details and parameters of the transmit and receive elements of the testbed are then given.

A. Signals

In total three types of OFDM signal are used. These are two types of long term evolution (LTE) signals: 'LTE 5 MHz', and, 'LTE 20 MHz', which are derived from the software simulator in [7], and a WiMAX signal derived from the the software simulator in [8]. The parameters of these signals are given in Table I. Each signal has a different length T_d and different CP size, T_c. The choice of modulation scheme in each OFDM sub-band is 16 QAM. The term, $M - T_d$, refers to the number of signal samples used in each autocorrelation calculation. $M - T_d$ is chosen judiciously in order to examine a complete snapshot of system behaviour over the range of SNRs in the testbed campaign. Increasing the value of $M - T_d$ can provide better performance in the low SNR region but this feature is not the focus of this work. F_s refers to the necessary sample rates that each of the signals requires [8] [9].

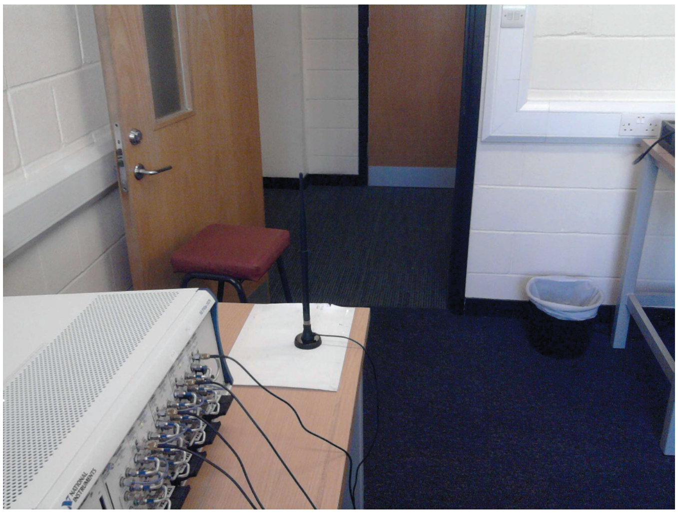

Fig. 2. Transmit chassis.

Fig. 3. Receive chassis.

B. Tx Chassis

The Tx chassis is shown in Fig. 2 and is similar to the one that appears in [10] [11]. It consists of a number of components, most notably a 4-channel radio frequency signal generator (RFSG) with antennas and an embedded PC controller. The 4-channel RFSG comprises a single RF local oscillator (LO), four arbitary waveform generators (AWGs) and four 6.6 GHz RF signal up-converters. The LO generates an RF reference signal and a 10 MHz reference clock that are shared by the four RF signal up-converters to enable synchronised transmission. The RFSG has an operational frequency range of 85 MHz to 6.6 GHz and can facilitate a bandwidth of 100 MHz at a max. Tx power of 10 dBm. The embedded PC controller is used to control the Tx and provides networking interfaces. It has an Intel qual-core i7 1.73 GHz processor and runs embedded Windows 7 as its operating system. Software that is used to interact with the Tx of the UC4G testbed, i.e. Labview and Matlab, is run from here.

Throughout the campaign, the position of the Transmit chassis is as depicted in Fig. 2, i.e. in a furnished laboratory room near the entrance door. The OFDM signals described in Section III-A are loaded into a Matlab vector before being written to a binary file, which the testbed can then transmit. The software in embedded PC controller of the Tx chassis allows the user to control the power, which was adjusted to provide Rx SNRs of -20 dB to 16 dB in steps of 3 dB.

C. Rx Chassis

The Tx chassis is shown in Fig. 3 and, again, is similar to the one that appears in [10] [11]. It consists of 2-channel RF signal analyser, which can be further broken down into several modules: a LO, two digitisers (ADs) and two 6.6 GHz RF signal down-converters. The LO generates an RF reference signal and a 10 MHz reference clock. Both the RF reference signal and the 10 MHz clock are shared by the two RF signal down-converters to enable synchronised reception. The four digitizers each have an on-board memory of 256 Mbytes to record RF data. The RFSA can operate in a frequency range of 10 MHz to 6.6 GHz and can facilitate an operational bandwidth of 50 MHz.

It is important to note the position of the Rx chassis in Fig. 3, i.e. in a corridor that is in proximity to the laboratory room where the transmit chassis is located. This was to ensure a non line of sight (somewhat realistic) channel. Again, the embedded PC in the Rx chassis can be used to set the Rx sampling frequency, which was matched to the Tx as 30 MSamples/sec. A total of 120 MSamples were recorded for each Rx SNR and each of the three signal types.

IV. Frequency Offset

One of the main impediments of the correct functioning of this algorithm is frequency offset. This can occur as a result of the Doppler effect but also occurs due to oscillator drifts. It comes in two forms known as fractional frequency offset (FFO) and integer frequency offset (IFO) [12]. To distinguish these, consider the sub-carrier spacing, Δf, which can be interpreted a measure of how much an OFDM signal would be shifted in the frequency domain. If the shift is some integer multiple, I, i.e., shifted $I\Delta f$, then this is referred to as a IFO. However if there is a shift δf Hz that is not an integer multiple of Δf then this is referred to a FFO. IFO has no effect on ρ but FFO on the other hand does affect ρ. To examine this, consider the effect of FFO on the receive signal $y\left(t\right)$ [13]:

$$y\left(t\right) = \exp\left\{j2\pi\frac{\delta f}{\Delta f T_d}t\right\}x\left(t\right) + n\left(t\right), \tag{6}$$

where $\delta f/\Delta f$ is the ratio of FFO to sub-band spacing, known as the 'normalised frequency error', which can be used to quantify the FFO. Eqn (6) now forms the basis for a simulation of the effect of FFO on ρ for the LTE 5 MHz and LTE 20 MHz OFDM signals for the case where $\delta f/\Delta f = 0.7$. The results of the simulation are given in Fig. 4.

It is clear from Fig. 4 that, for the case where there is no FFO, the curves for LTE 5 MHz and LTE 20 MHz are more or less identical. This is reasonable since in theory ρ at lag: T_d, is given by the term: $\left(T_c/\left(T_d+T_c\right)\right)\left(SNR/\left(1+SNR\right)\right)$ and careful inspection of Table I reveals this quantity to be equivalent. However, what is more significant is the fact that

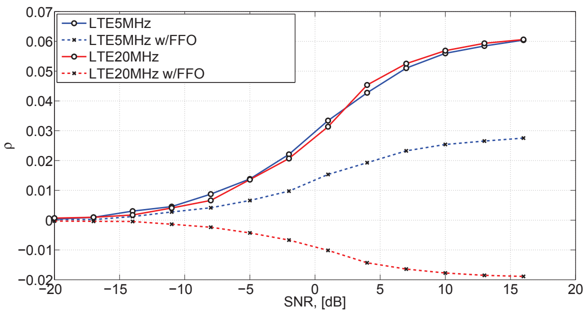

Fig. 4. Simulation of the effect of FFO on on ρ for LTE 5 MHz and LTE 20 MHz OFDM signals for $\delta f/\Delta f = 0.7$

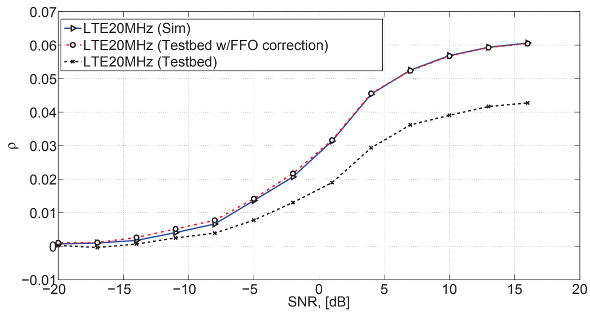

Fig. 5. Values of ρ derived from simulation, testbed and FFO corrected testbed receive signals. Simulation and FFO corrected curves are on top of one another.

the effect of an equivalent degree of FFO is more dramatic in the case of LTE 20 MHz than for that of LTE 5 MHz. Thus performing an autocorrelation-based spectrum sensing on signals with large values of T_d (or larger FFT size) and a given degree of FFO could give rise to more significant performance loss. Therefore in order to detect OFDM signals with longer T_d, it is necessary to compensate for FFO in an appropriate manner. In relation to this, the effect of FFO on the autocovariance of $y(t)$, i.e., $\mathbb{E}\{y(t)\,y^*(t+\Delta t)\}$, may be summarised as follows [14] [15]:

$$\varphi = \mathbb{E}\{y(t)\,y^*(t+\Delta t)\} = \begin{cases} \sigma_x^2 + \sigma_n^2 & \Delta t = 0 \\ \sigma_x^2 \exp\{j2\pi\delta f\} & \Delta t = T_d \\ 0 & \text{otherwise} \end{cases} \tag{7}$$

$\mathbb{E}\{\cdot\}$ is the expectation operator and when the lag, Δt, corresponds to T_d, it can be deduced that FFO causes a rotation in φ. Comparing eqns (2) and (7) appropriately and relaxing the use of $\mathbb{E}\{\cdot\}$ to an appropriately scaled summation, φ can be set: $\varphi = \frac{1}{2M}\sum_{t=0}^{M-1}\Re\{y(t)\,y^*(t+T_d)\}$ for the case where the lag is T_d and thus, it is possible to write:

$$\rho = \frac{\frac{1}{2M}\sum_{t=0}^{M-1}\Re\{\varphi\}}{\frac{1}{2M+T_d}\sum_{t=0}^{M+T_d-1}|y(t)|^2}. \tag{8}$$

Since only the real part of φ is used to determine ρ, a rotation in φ could have a detrimental effect on ρ if the extent of the FFO, δf, were significant enough. To correct for this, it is proposed that N calculations $\varphi_1, \varphi_2, ..., \varphi_N$ be made and buffered. Then for each buffered value, the respective complex phase angles, $\theta_{\varphi_{(1)}}, \theta_{\varphi_{(2)}}, ..., \theta_{\varphi_{(N)}}$, can be calculated. From this, the mean value of θ_φ, i.e., $\frac{1}{N}\sum_{n=1}^{N}\theta_{\varphi_{(n)}}$, is obtained to form a correction factor. This factor that can then be applied to all of the calculations of ρ in the manner:

$$\rho = \frac{\frac{1}{2M}\sum_{t=0}^{M-1}\Re\left\{\varphi\exp\left\{-j\frac{1}{N}\sum_{n=1}^{N}\theta_{\varphi_{(n)}}\right\}\right\}}{\frac{1}{2M+T_d}\sum_{t=0}^{M+T_d-1}|y(t)|^2}. \tag{9}$$

Finally, it should be clarified that too low a value of N would change the statistical character of ρ in eqn (9), which would thus negate the statistical framework used to evaluate the threshold in eqn (5).

V. Implementation and Simulation Results

The simulation and testbed implementation of the three OFDM signals in Table I are now compared. Firstly, in Fig. 5, the values of ρ derived from simulation and testbed are compared for the case of LTE 20 MHz, since it is expected that for this particular signal, the effect of FFO correction would be the most dramatic by comparison with the rest of the signals. The curve 'testbed w/FFO correction', incorporates the FFO correction procedure discussed in Section IV. It is clear that there is a closer match to the simulation results when the FFO has been corrected.

Further to this, the probability of detection, P_d, is now considered for the three OFDM signals in Figs. 6, 7 and 8, for a probability the false alarm, $P_{fa} = 0.1$. In all cases, 2000 autocorrelations were performed, each using $M - T_d$ samples for calculation. For FFO correction, N was set $N = 50$, which is a trade-off between sensing time and better performance. A comparison of the sensing times as a result of applying this improvement may be made by careful inspection of the last two rows of Table I. As expected from Fig.5 and indeed from Fig. 4, in Section IV, the effect of FFO correction has the most dramatic effect on the results pertaining to LTE 20 MHz. For the cases of LTE 5 MHz and WiMAX signals, there is a reasonable match between simulation and testbed performance regardless of whether FFO correction was applied.

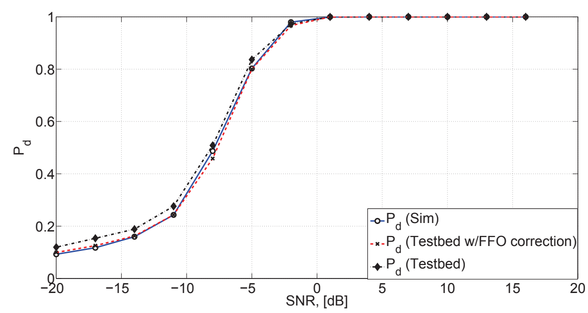

Fig. 6. P_d for WiMAX signals for the case of simulation, testbed and testbed with FFO correction. $P_{fa} = 0.1$. Sensing time: 0.255 ms, w/FFO correction: 12.5 ms

VI. Conclusions

This work described an implementation of an autocorrelation-based spectrum sensing algorithm that

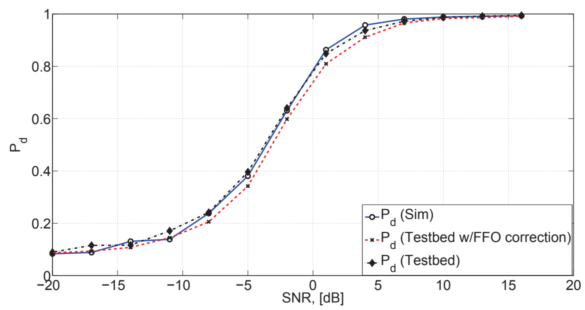

Fig. 7. P_d for LTE 5 MHz signals for the case of simulation, testbed and testbed with FFO correction. $P_{fa} = 0.1$. Sensing time: 0.347 ms, w/FFO correction: 17.4 ms

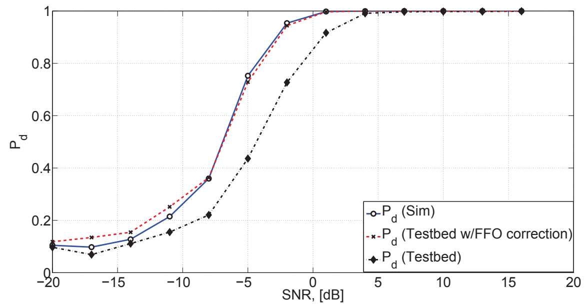

Fig. 8. P_d for LTE 20 MHz signals for the case of simulation, testbed and testbed with FFO correction. $P_{fa} = 0.1$. Sensing time: 0.347 ms, w/FFO correction: 17.4 ms

can detect various OFDM signal types based on the FFT size (T_d). This contribution is an extension to the implementation-based work of other authors [5] to the case of larger FFT sizes where the algorithm would ordinarily fail due to the hardware effect of FFO. A novel method for correcting the effect of FFO on the functioning of this algorithm has been proposed and as a result a better match between simulation and experimental implementation results was observed due to this improvement. A reasonable portion of this FFO correction based algorithm improvement is already being used in OFDM receivers for another related purpose so the performance improvement exhibited here would merely be a trade-off between increased sensing time as well as computational buffering effort. Therefore, the increased complexity is not thought to be prohibitive.

Acknowledgments

The authors would like to thank University Defence Research Centre (UDRC) and Dr. Simon Angove Defence Science and Technology Laboratory (DSTL) for funding the work. The authors also would like to thank Prof. C-X Wang of Heriot-Watt University for providing access to the wireless testbed used in this work and Dr. Bassem Zayen, formerly of TELECOM ParisTech/Eurecom and now with AMESYS-Intel Mobile Communications, for valuable discussions concerning the algorithm.

References

[1] H. Urkowitz, “Energy detection of unknown deterministic signals,” in *Proc. IEEE*, vol. 55, no. 4, April 1967, pp. 2355–2369.

[2] S. Chaudhari, J. Lunden, and V. Koivunen, “Collaborative autocorrelation-based spectrum sensing of OFDM signals in cognitive radios,” in *Proc. 42nd Annual Conference on Information Sciences and Systems, 2008. (CISS 2008)*, Mar 2008, pp. 191–196.

[3] S. Chaudhari, V. Koivunen, and H. Poor, “Distributed autocorrelation-based sequential detection of OFDM signals in cognitive radios,” in *Proc. 3rd International Conference on Cognitive Radio Oriented Wireless Networks and Communications, 2008. (CrownCom 2008)*, May 2008, pp. 1–6.

[4] B. Zayen, “Spectrum sensing and resource allocation strategies for cognitive radio,” Ph.D. dissertation, TELECOM ParisTech/Eurocom, 2010. [Online]. Available: http://pastel.archives-ouvertes.fr/docs/00/57/64/59/PDF/Rapport_de_these_Bassem_Zayen.pdf

[5] K. Kokkinen, V. Turunen, M. Kosunen, S. Chaudhari, V. Koivunen, and J. Ryynänen, “On the implementation of autocorrelation-based feature detector,” in *Proc. 4th international symposium on communications, control and signal processing 2010 (ISCCSP 2010)*, Mar 2010.

[6] S. Chaudhari, V. Koivunen, and H. V. Poor, “Autocorrelation-based decentralisation sequential detection of OFDM signals in cognitive radios,” *IEEE Trans. Signal Process*, vol. 57, no. 7, July 2009.

[7] C. Mehlführer, J. C. Ikuno, M. Šimko, S. Schwarz, M. Wrulich, and M. Rupp, “The vienna LTE simulators - Enabling reproducibility in wireless communications research,” *EURASIP Journal on Advances in Signal Processing 2011*, July 2011.

[8] C. Mehlführer, S. Caban, and M. Rupp, “Experimental evaluation of adaptive modulation and coding in MIMO WiMAX with limited feedback,” *EURASIP Journal on Advances in Signal Processing, Special Issue on MIMO Systems with Limited Feedback*, vol. 2008, Article ID 837102, 2008. [Online]. Available: http://publik.tuwien.ac.at/files/pub-et_13762.pdf

[9] S. Sesia, I. Toufik, and M. Baker, *LTE-The UMTS Long Term Evolution: From Theory to Practice*. Wiley, 2009.

[10] P. Chambers, X. Hong, Z. Chen, C.-X. Wang, M. Beach, and H. Haas, “The UC4G wireless MIMO testbed,” in *Proc. Global Communications Conference (GLOBECOM)*, Dec 2012, pp. 4368–4373.

[11] N. Serafimovski, A. Younis, R. Mesleh, P. Chambers, M. DiRenzo, C.-X. Wang, M. Beach, and H. Haas, “Practical implementation of spatial modulation,” *IEEE Trans. Wireless Commun.*, vol. 62, no. 9, pp. 4511–4523, Nov 2013.

[12] T. Keller and L. Hanzo, “Adaptive multicarrier modulation: a convenient framework for time-frequency processing in wireless communications,” *Proc. IEEE*, vol. 88, no. 5, pp. 611–640, May 2000.

[13] L. Rugini and P. Banelli, “BER of OFDM systems impaired by carrier frequency offset in multipath fading channels,” *IEEE Trans. Wireless Commun.*, vol. 4, no. 5, pp. 2279–2288, Sept 2005.

[14] J.-J. van de Beek, M. Sandell, and P. Börjesson, “ML estimation of time and frequency offset in OFDM systems,” *IEEE Trans. Signal Process*, vol. 45, no. 7, July 1997.

[15] P. H. Moose, “A technique for orthogonal frequency division multiplexing frequency offset correction,” *IEEE Trans. Commun*, vol. 42, no. 10, Oct 1994.